THE JOURNAL OF BIOLOGICAL CHEMISTRY
Vol. 278, No. 52, Issue of December 26, pp. 52700–52709, 2003
Printed in U.S.A.

Cell Surface Expression of GluR5 Kainate Receptors Is Regulated by an Endoplasmic Reticulum Retention Signal*

Received for publication, August 28, 2003, and in revised form, October 3, 2003
Published, JBC Papers in Press, October 3, 2003, DOI 10.1074/jbc.M309585200

Zhao Ren‡, Nathan J. Riley‡, Leigh A. Needleman§, James M. Sanders¶, Geoffrey T. Swanson¶, and John Marshall‡‖

From the ‡Department of Molecular Pharmacology, Physiology and Biotechnology and §Department of Neuroscience, Brown University, Providence, Rhode Island 02912 and the ¶Department of Pharmacology and Toxicology, University of Texas Medical Branch, Galveston, Texas 77555

Kainate receptors (KARs) are mediators of excitatory neurotransmission in the mammalian central nervous system, and their efficient targeting and trafficking is critical for normal synaptic function. A key step in the delivery of KARs to the neuronal plasma membrane is the exit of newly assembled receptors from the endoplasmic reticulum (ER). Here we report the identification of a novel ER retention signal in the alternatively spliced C-terminal domain of the GluR5–2b subunit, which controls receptor trafficking in both heterologous cells and neurons. The ER retention motif consists of a critical arginine (Arg-896) and surrounding amino acids, disruption of which promotes ER exit and surface expression of the receptors, as well as altering their physiological properties. The Arg-896-mediated ER retention of GluR5 is regulated by a mutation that mimics phosphorylation of Thr-898, but not by PDZ interactions. Furthermore, two positively charged residues (Arg-900 and Lys-901) in the C terminus were also found to regulate ER export of the receptors. Taken together, our results identify novel trafficking signals in the C-terminal domain of GluR5–2b and demonstrate that alternative splicing is an important mechanism regulating KAR function.

Kainate, NMDA,[1] and AMPA receptors mediate glutamatergic excitatory neurotransmission in the mammalian central nervous system (1, 2). The intracellular trafficking and surface delivery of multimeric transmembrane proteins, such as kainate receptors, are likely to be tightly controlled processes requiring proper folding and assembly of constituent subunits, so that only fully assembled, functional receptors can be expressed on the plasma membrane. The endoplasmic reticulum (ER) is the primary checkpoint for these complex events (3). Recently, we demonstrated that an arginine-rich ER retention signal controls the ER egress and surface expression of KA2 kainate receptor subunits (4).

Alternative splicing and RNA editing of ionotropic glutamate receptors have been shown to play important roles in receptor assembly and trafficking (5–8). In particular, an R*X*R (where R is arginine and *X* a large neutral or positively charged residue) motif was found in the alternatively spliced C1 cassette in the C terminus of NMDA receptor NR1 subunit, mediating the intracellular retention of most C1-containing NR1 isoforms (6, 7). Furthermore, this R*X*R-mediated ER retention was regulated by protein kinase C (PKC) phosphorylation (6) and a type I PDZ (postsynaptic density-95/Disc large/zona occludens-1)-binding motif in the alternate C2′ splice cassette (6, 7). In addition, arginine 607 (Arg-607) at a Q/R (glutamine/arginine) mRNA editing site has been reported to determine the ER retention of GluR2 AMPA receptor subunits in cultured neurons (8).

The GluR5 kainate receptor subunit also undergoes alternative splicing and RNA editing. Alternative splicing of the N-terminal region of the rat GluR5 mRNA yields two different isoforms, GluR5–1 and GluR5–2, where GluR5–1 contains an extra 15 amino acids compared with GluR5–2 (9). In addition, GluR5–2 has three splice variants in the C terminus, named GluR5–2a, GluR5–2b, and GluR5–2c (9, 10). The shortest isoform, GluR5–2a, results from the introduction of a stop codon after 2 amino acids in the alternatively spliced cassette (10), whereas the longest variant, GluR5–2c, is generated by an in-frame insertion of nucleotides, coding for an additional 29 amino acids, into the GluR5–2b sequence (10). GluR5–2b and GluR5–2c share a C-terminal consensus type I PDZ-binding domain that is absent in GluR5–2a. Although RNA editing of GluR5 is known to modulate its single-channel conductance, calcium permeability, and rectification properties (10, 11), the functional significance of these splice variants remains to be defined.

In the present study, we investigated the intracellular trafficking and surface expression of the GluR5 splice variants, GluR5–2a and GluR5–2b. We now report the identification of a novel ER retention signal present in the alternatively spliced C-terminal domain of GluR5–2b. This signal consists of a critical Arg-896 and surrounding residues, disruption of which promotes ER exit and surface delivery of GluR5–2b receptors in both heterologous cells and hippocampal neurons. In addition, a pair of positively charged residues in the C-terminal region, Arg-900 and Lys-901, were found to regulate ER export of the receptors. Together, our results demonstrate the functional

* This work was supported by Grants NS39309 and NS39063 from the National Institutes of Health (to J. M.), Grant 9940131N from the American Heart Association (to J. M.), Centers of Biomedical Research Excellence (COBRE) Grant RR15578 (to J. M.), a National Institute on Drug Abuse predoctoral award (to J. M. S.), and Grants MH065289 from the National Institute of Mental Health and NS44322 from NINDS, National Institutes of Health (to G. T. S.). The costs of publication of this article were defrayed in part by the payment of page charges. This article must therefore be hereby marked "*advertisement*" in accordance with 18 U.S.C. Section 1734 solely to indicate this fact.

‖ To whom correspondence should be addressed: Dept. of Molecular Pharmacology, Physiology, and Biotechnology, Brown University, Box G-B4, Providence, RI 02912. Tel.: 401-863-2574; Fax: 401-863-1595; E-mail: john_marshall@brown.edu.

[1] The abbreviations used are: NMDA, *N*-methyl-D-aspartate; AMPA, α-amino-3-hydroxy-5-methyl-4-isoxazolepropionic acid; ER, endoplasmic reticulum; HEK, human embryonic kidney; KAR, kainate receptor; endo H, endoglycosidase H; DMEM, Dulbecco's modified Eagle's medium; GFP, green fluorescent protein; NHS, *N*-hydroxysulfosuccinimide; FITC, fluorescein isothiocyanate; TBS, Tris-buffered saline; PBS, phosphate-buffered saline; PNGase F, peptide-*N*-glycosidase F; PKC, protein kinase C; PKA, protein kinase A; FAC, flow-assisted cytometry.

significance of GluR5 alternative splicing and identify ER retention as an important mechanism regulating kainate receptor trafficking and surface expression.

EXPERIMENTAL PROCEDURES

Cell Culture—Human embryonic kidney 293 (HEK293) cells, normal rat kidney (NRK) cells, and COS7 cells (ATCC, Manassas, VA) were grown in DMEM (Invitrogen) supplemented with 10% fetal bovine serum and 50 units/ml penicillin and streptomycin (37 °C, 5% CO_2). For immunocytochemistry experiments, cells were plated onto poly-D-lysine-coated glass coverslips in the same growth medium. Primary cultures of hippocampal neurons were obtained from E18 rat embryos. Briefly, hippocampi were dissected from E18 Sprague-Dawley rats and dissociated with trypsin. Dissociated cells were then plated onto poly-L-lysine (Sigma)-coated glass coverslips at a density of 7500 cells/cm^2 in Neurobasal medium (Invitrogen) supplemented with Glutamax and B27. Arabinofuranosyl-cytosine (5 μM) was added 3 days after plating, and cells were fed twice weekly thereafter.

Molecular Biology—The pMLSV N1/N4 expression vector for human Tac was purchased from ATCC. The Tac coding sequence was then amplified by PCR and subcloned into a HindIII-XbaI site in pcDNA3. To generate the Tac-GluR5 and Tac-GluR6 chimeras, we first amplified the N-terminal and transmembrane sequences of Tac, as well as the C termini of GluR5/2a, GluR5–2b, and GluR6 by PCR, then ligated both fragments into a HindIII-XbaI site in pcDNA3 vector after digestion. Deletion mutants of Tac-G5/2b were made by PCR amplification of the desired sequences and subsequent subcloning into the HindIII-XbaI site in pcDNA3 expression vector. Tac-G5/2b and Tac-G6 point mutations were also made by PCR. GluR5–2a-pRK5 and GluR5–2b-pBluescript SK(−) were generous gifts from Dr. Peter Seeburg (Max Planck Institute for Medical Research, Heidelberg, Germany) and Dr. Steve Heinemann (Salk Institute, La Jolla, CA), respectively. To make GFP-GluR5–2b in pRK5 expression vector, we first replaced a C-terminal BamHI-EcoRI fragment in GluR5–2a-pRK5 with the corresponding piece from GluR5–2b amplified by PCR. The GFP coding sequence was then amplified by PCR from pEGFP-C2 vector (BD Biosciences, San Jose, CA) and inserted after residue 36 (counted from the initiator methionine) of GluR5–2b in pRK5, using an XhoI site created by QuikChange (Stratagene, La Jolla, CA). The pDsRed2-ER vector was purchased from BD Biosciences. Myc-tagged PICK1 (protein interacting with C kinase) and GRIP1a (glutamate receptor interacting protein) in pRK5 vector were gifts from Dr. Richard Huganir (Johns Hopkins University, Baltimore, MD), and PSD-95-pGW1 (postsynaptic density-95) was a gift from Dr. Morgan Sheng (Massachusetts Institute of Technology, Cambridge, MA). All the mutagenesis and PCR-derived sequences were sequenced for verification.

Transfection—HEK293, COS7, and NRK cells were transfected using FuGENE 6 transfection reagent (Roche Molecular Biochemicals), following the manufacturer's protocol for transient transfection of adherent cells. Cultured hippocampal neurons (DIV7) were transfected with the LipofectAMINE 2000 transfection reagent (Invitrogen), using the protocol from the manufacturer. Surface and intracellular protein expressions were analyzed 48 h after transfection.

Antibodies—Monoclonal anti-Tac (Covance, Princeton, NJ) was used at 1:800 or 1:2000 for immunostaining of heterologous cells or hippocampal neurons, and 1:4000 for flow cytometry. Polyclonal anti-Tac (Santa Cruz Biotechnology, Santa Cruz, CA) was used at 1:200 for staining and 1:300 for Western blots. Monoclonal anti-TGN38 (Calbiochem, San Diego, CA), anti-mannosidase II (Covance), and polyclonal anti-giantin (Covance) were used at 1:1000 for immunofluorescence of heterologous cells. Polyclonal anti-calnexin (Stressgen, Victoria, British Columbia, Canada) and anti-GFP (Santa Cruz Biotechnology) were used at 1:200 for immunostaining. Monoclonal anti-autofluorescent protein antibody (Qbiogene, Carlsbad, CA) was used at 1:200 for immunofluorescence and 1:500 for flow cytometry. Monoclonal anti-GFP (B-2) antibody (Santa Cruz Biotechnology) was used at 1:300 for Western blots. Polyclonal anti-GluR5 (Upstate Biotechnology, Inc., Lake Placid, NY) was used at 1:100 for immunofluorescence and 1:1000 for Western blots. Monoclonal anti-PSD-95 (Upstate Biotechnology, Inc.) and anti-Myc (Santa Cruz Biotechnology) were used at 1:100,000 and 1:250, respectively, for Western blots. All secondary antibodies conjugated to fluorescein (FITC), phycoerythrin, or rhodamine red-X (Jackson Immunoresearch, West Grove, PA) were used at 1:200 for immunostaining. All secondary antibodies conjugated to horseradish peroxidase (BD Biosciences) were used at 1:10,000 for Western blot.

Protein Preparation and Immunoblotting—Forty-eight hours after transfection, HEK cells grown in 60-mm culture dishes were washed once with cold TBS and homogenized in 1 ml of lysis buffer (1% Triton X-100 in TBS with 0.1 mM phenylmethylsulfonyl fluoride, 10 μg/ml aprotinin, 10 μg/ml leupeptin, 10 μg/ml pepstatin A, 2 mM EDTA, pH 8.0). The samples were then solubilized for 1 h at 4 °C and cleared by centrifugation at 14,000 × *g* for 30 min. Aliquots of the supernatants were boiled for 5 min in 1× sample buffer and resolved on 8% or 10% SDS-PAGE. Gels were then Western blotted, immunostained, and visualized with Supersignal West Pico chemiluminescent substrate (Pierce).

Biotinylation of Cell Surface Protein—Transfected HEK cells, grown in poly-D-lysine-coated 60-mm culture dishes, were washed three times with ice-cold PBS and incubated 15 min with 1.0 mg/ml EZ-link™ sulfo-*N*-hydroxysulfosuccinimide (NHS)-S-S-biotin (Pierce) in cold PBS, pH 8.0, with gentle agitation at 4 °C. Cells were washed once and incubated with a quenching buffer (192 mM glycine, 25 mM Tris in PBS) for 10 min. Next, cells were rinsed twice in cold PBS, collected, homogenized in lysis buffer, and centrifuged. Supernatants were then incubated with 50 μl of 50% slurry of streptavidin-Sepharose beads (Amersham Biosciences) for 2 h at 4 °C. Beads were pelleted by brief centrifugation, and aliquots of the supernatant were taken to represent the unbound, intracellular pool. Beads were then washed three times with lysis buffer, and biotinylated proteins were eluted by boiling in 1× sample buffer for 5 min, separated by SDS-PAGE, and immunoblotted as above.

Immunofluorescence—For selective labeling of surface receptors, transfected live COS7 cells were incubated with appropriate primary antibodies (monoclonal anti-Tac or anti-autofluorescent protein) diluted in DMEM supplemented with 5% fetal bovine serum for 1 h at 4 °C. The cells were then washed with cold PBS and fixed with 4% paraformaldehyde and 4% sucrose on ice for 20 min. After fixation, cells were washed with PBS and labeled with fluorescence-conjugated secondary antibodies. Next, cells were permeabilized at room temperature with 0.2% Triton X-100 for 5 min. Intracellular expression was then determined by sequentially incubating with a second set of primary (polyclonal anti-Tac or anti-GFP) and secondary antibodies. A slightly modified protocol was used for staining transfected hippocampal neurons. Briefly, for surface labeling, cultured live neurons were incubated with anti-Tac diluted in PBS with 5% normal goat serum for 30 min at room temperature, fixed, and incubated with a rhodamine-conjugated anti-mouse secondary antibody. To detect intracellular expression, neurons were then permeabilized and sequentially incubated with anti-Tac and FITC-conjugated anti-mouse secondary antibody diluted in PBS with 10% normal goat serum. Both surface and intracellular expression were visualized on a Axioskop fluorescence microscope (Zeiss, Thornwood, NY) coupled to a CCD camera (Hamamatsu, Hamamatsu City, Japan) and analyzed by OpenLab imaging software (Improvision, Coventry, United Kingdom). Colocalization images were obtained with the permeabilized staining protocol, visualized with a Zeiss LSM410 confocal microscope (Zeiss), and analyzed with Renaissance imaging software (Microcosm, Columbia, MD).

Flow-assisted Cytometry—Transfected live HEK293 cells grown in 6-well tissue culture plates were incubated with monoclonal anti-Tac or anti-Myc antibodies diluted in DMEM supplemented with 5% serum for 1 h at 4 °C. Cells were then washed with PBS and incubated with FITC- or phycoerythrin-conjugated anti-mouse secondary antibodies in PBS for 1 h at 4 °C. After extensive washing, cells were detached from the plates with 500 μl of PBS plus 5 mM EDTA, and transferred to 12 × 75-mm polystyrene test tubes (VWR Scientific, South Plainfield, NJ). Finally, 500 μl of 4% paraformaldehyde in PBS was added to fix the cells. Surface expression was quantified using a FACScalibur cell sorter (BD Biosciences). Background fluorescence was determined using mock-transfected HEK293 cells incubated with corresponding primary and secondary antibodies. Mean fluorescence intensity was acquired and plotted with Prism4.0 software (GraphPad, San Diego, CA).

In Vitro Deglycosylation—Transfected HEK cells grown in 35-mm dishes were washed with ice-cold TBS and homogenized in 1 ml lysis buffer (0.1% SDS, 5% deoxycholate and 1% Nonidet P-40 in TBS, plus 2 mM EDTA, 0.1 mM phenylmethylsulfonyl fluoride, 1 μg/ml pepstatin A, 1 μg/ml chemostatin, and 1 μg/ml leupeptin, pH 8.0). After brief sonication and centrifugation (14,000 rpm for 20 min at 4 °C), the supernatants were collected. 6 μl of Denature Buffer (New England Biolabs, Beverly, MA) was added to 54 μl of cell lysate. The samples were then boiled for 10 min, divided into thirds, and treated with 500 units of peptide-*N*-glycosidase F (PNGase F; New England Biolabs), 500 units of endoglycosidase H (endo H; New England Biolabs), or no enzyme for 5 h at 37 °C. After incubation, samples were boiled for 5 min in 1× sample buffer, resolved on 10% SDS-PAGE, and immunoblotted as described.

Kinase Activation Experiments—HEK cells transfected with Tac-

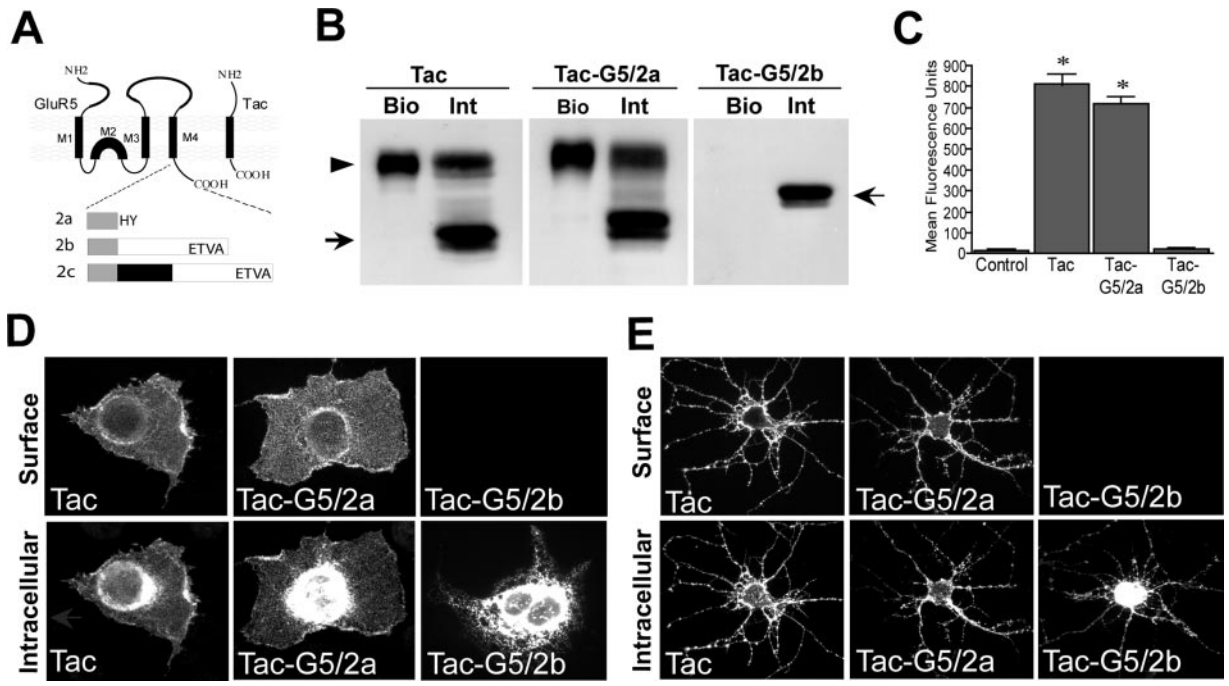

FIG. 1. **The C terminus of GluR5–2b contains intracellular retention signal(s).** *A*, schematic diagram illustrating the structures of three GluR5 splice variants and Tac. *Top panel*, the topology of GluR5 and Tac. GluR5 has four membrane-spanning segments marked by M1–4, whereas Tac has a single transmembrane domain, with a long N-terminal region and a short C-terminal tail. *Bottom panel*, schematic representation of the C termini of three GluR5 splice variants. The proximal cassette (*gray bar*) is in all isoforms, whereas the distal cassette (*white bar*) that contains a PDZ-binding motif (ETVA) is only present in GluR5–2b and 2c. GluR5–2c has an extra inserted sequence (*black bar*). *B*, surface expression of Tac and Tac-G5 chimeras evaluated by biotinylation. Transfected live HEK293 cells were surface biotinylated with sulfo-NHS-S-S-biotin, the biotinylated (*Bio*) and intracellular (*Int*) fractions of cell extract were purified and immunoblotted with anti-Tac antibody. The mature forms of Tac (*left panel*, *first lane*) and Tac-G5/2a (*middle panel*, *first lane*) are present in the biotinylated fractions. Tac-G5/2b only exists as an immature form (*right panel*, *second lane*), with no signal in the biotinylated fraction (*right panel*, *first lane*). *Arrows* designate immature Tac and Tac-G5 species, whereas *arrowhead* designates mature forms. *C*, flow cytometric quantification of surface expression of Tac and Tac-G5 chimeras in HEK293 cells. Data represent means ± S.E. of fluorescence intensities from 50,000 cells stained for surface expression of Tac or chimeras (*, $p < 0.05$ relative to mock-transfected control, by Student's unpaired *t* test). *D*, surface and intracellular expression of Tac and Tac-G5 chimeras in COS7 cells. Tac and Tac-G5/2a showed robust surface expression, but no surface staining could be detected for TacG5/2b. *E*, staining of the same constructs expressed in the hippocampal neurons shows identical patterns as in COS7 cells.

G5/2b were treated with (*a*) 100 nM phorbol 12-myristate 13-acetate in Me_2SO for 30 min, washed with fresh media, and allowed to recover at 37 °C for 3 h; (*b*) 50 μM forskolin together with 10 μM phosphodiesterase inhibitor, isobutylmethylxanthine, in Me_2SO for 2 h; or (*c*) Me_2SO only. Cells were then examined for surface expression as by flow-assisted cytometry (FAC) analysis. Transfected COS cells were treated similarly; surface and intracellular expression of the receptors were then examined by live immunostaining as described. All experiments were done in a blind manner.

Electrophysiology—HEK293 cells were plated on glass coverslips coated with 100 μg/ml collagen and poly-D-lysine. The following day, cells were transfected with plasmids containing the wild type or mutant GFP-GluR5–2b (0.2 μg/coverslip) using FuGENE 6 transfection reagent according to the instructions from the manufacturer. Whole-cell patch clamp recordings were made with an Axopatch 200B amplifier (Axon Instruments, Foster City, CA) 2–3 days after transfection. The external bath solution contained 150 mM NaCl, 2.8 mM KCl, 10 mM glucose, 2 mM $CaCl_2$, 1.0 mM $MgCl_2$, and 10 mM HEPES (pH was adjusted to 7.3 with NaOH). The internal solution was composed of 110 mM CsF, 30 mM CsCl, 4 mM NaCl, 0.5 mM $CaCl_2$, 10 mM HEPES, and 5 mM EGTA (adjusted to pH 7.3 with CsOH). For rapid agonist application, cells were lifted from the coverslip into a laminar solution stream exiting a three-barrel glass pipette (Vitro Dynamics, Rockaway, NJ) pulled to an internal barrel diameter of ~80 μm and mounted on a piezo-ceramic bimorph. The solution stream was rapidly moved across the transfected cells by applying voltage to the bimorph with a stimulation-isolation unit triggered by a digital signal from pClamp 8 software. Data were acquired and analyzed using pClamp 8 software (Axon Instruments, Foster City, CA) and Origin 6.0 (OriginLab Corp., Northampton, MA).

RESULTS

GluR5–2b C-terminal Domain Contains an Intracellular Retention Signal—The distinct C-terminal sequences of GluR5 splice variants (Fig. 1*A*) are known to be responsible for their differential interactions with intracellular scaffolding molecules (12), however their roles in receptor trafficking remain unexplored. To facilitate the search for potential trafficking signals in these alternatively spliced C termini and to avoid the complication of assembly with native subunits in neurons, we constructed chimeric receptors consisting of the N-terminal and transmembrane domains of the human interleukin-2 receptor α subunit (Tac), and the C terminus of either GluR5–2a or GluR5–2b (designated Tac-G5/2a and Tac-G5/2b, respectively) (Fig. 1*A*).

The expression profiles of the Tac-G5 chimeras and Tac alone were then examined in HEK cells with a biotinylation method using sulfo-NHS-S-S-biotin. Because this modified biotin is membrane-impermeable, it only binds to surface proteins, which can then be separated from the intracellular pool by conjugation with streptavidin beads and visualized by Western blotting. Using this method, we observed strong surface expression of Tac and Tac-G5/2a (Fig. 1*B*), whereas Tac-G5/2b signal could not be detected on the plasma membrane, despite its robust intracellular expression (Fig. 1*B*). Furthermore, the intracellular Tac was present as both a high molecular mass (55 kDa) and a low molecular mass (45 kDa) form (Fig. 1*B*), but only the high molecular mass species was detected in the biotinylated surface fraction (Fig. 1*B*). This is consistent with previous studies demonstrating that Tac is synthesized as a 45-kDa immature form in the ER and further processed upon transport into the Golgi apparatus, resulting in a shift of molecular mass (13, 14). The same pattern was also observed for Tac-G5/2a (Fig. 1*B*), whereas Tac-G5/2b could only be detected

as a low molecular mass species (Fig. 1*B*). The lack of a mature form for Tac-G5/2b suggests that it is unable to exit the early secretory compartments that include ER and ER-Golgi intermediate compartment (ERGIC). To quantify receptor surface expression, we performed a FAC analysis on HEK293 cells transfected with Tac or Tac-G5 receptors. Cells expressing Tac or Tac-G5/2a had 70-fold higher surface fluorescence compared with that of Tac-G5/2b (Fig. 1*C*). In all cases, total protein abundance of different receptors was comparable, as revealed by Western blot analyses of whole cell extracts (data not shown).

To confirm the intracellular retention of Tac-G5/2b, we employed a live immunofluorescence technique to visualize surface receptors. In agreement with the biotinylation and FAC data, Tac-G5/2b was not found on the plasma membrane, but rather retained intracellularly in a mesh network-like intracellular compartment reminiscent of ER morphology, with most of the staining concentrated in the perinuclear region (Fig. 1*D*). In contrast, Tac and Tac-G5/2a were readily detectable on the cell surface (Fig. 1*D*). Finally, to determine whether the intracellular retention of Tac-G5/2b receptor occurs in neurons, we transfected cultured hippocampal neurons with the Tac-G5 chimeras and analyzed their surface expression. As in the HEK and COS cells, Tac-G5/2b was retained inside the neurons, whereas both Tac and Tac- GluR5/2a were efficiently delivered to the neuronal surface (Fig. 1*E*). Together these data indicate that the C-terminal domain of GluR5–2b contains signal(s) sufficient to confer intracellular retention of Tac receptors in both heterologous cells and neurons.

Tac-G5/2b Receptors Are Retained in the ER—The two major intracellular organelles involved in protein biogenesis and trafficking are the ER and Golgi apparatus, both of which have distinctive morphology and unique molecular markers. To determine the precise intracellular location of the retained Tac-G5/2b receptor, we compared its distribution profile with those of the ER and Golgi markers. When expressed in COS7 or NRK cells, Tac-G5/2b colocalized extensively with the ER markers, calnexin and DsRed-ER (Fig. 2*A*), while showing no overlap with the Golgi proteins, giantin, mannosidase II, and TGN-38 (Fig. 2*B*).

Furthermore, in agreement with the earlier observation that Tac-G5/2b failed to reach the Golgi apparatus for post-translational processing (Fig. 1*B*), the receptor remained sensitive to endo H (Fig. 2*C*), an enzyme that preferentially hydrolyzes the high mannose *N*-glycans present on immature proteins in the ER (15). In contrast, Tac and Tac-G5/2a were resistant to endo H (Fig. 2*C*), indicating that these receptors had been processed in the Golgi, a result consistent with their strong surface expression (Fig. 1, *B–E*). To ensure that endo H-mediated deglycosylation was selective for Tac-G5/2b, we used PNGase F, a less selective glycosidase that cleaves most asparagine-bound glycans (16). Indeed, all the receptors exhibited increased electrophoretic mobility, indicating PNGase F sensitivity (Fig. 2*C*). These experiments provide both immunocytochemical and biochemical evidence for the selective ER retention of Tac-G5/2b receptors.

Arg-896 Is Critical for the ER Retention of Tac-G5/2b—The C terminus of GluR5–2b contains a number of arginine- and lysine-rich sequences, but no regions that match previously identified ER retention signals. To map the residue(s) conferring ER retention of Tac-G5/2b, we first made a series of deletional mutations (Fig. 3*A*), based on the positions of these arginine- and lysine-rich sequences, and examined their effects on ER retention. Deletion of the last 10 amino acids (Tac-G5/2bΔ10), but not the last 6 residues (Tac-G5/2bΔ6), effectively released Tac-G5/2b from ER retention in both COS7 cells (Fig. 3*B*) and hippocampal neurons (Fig. 3*C*). In contrast to Tac-G5/2b and Tac-G5/2bΔ6, Western blot analyses showed that Tac-G5/2bΔ10 was present as both mature and immature forms, providing biochemical evidence for its egress from ER (Fig. 3*D*). Quantification of surface expression using FAC indicated that the Tac-G5/2bΔ10 mutant had 35-fold greater surface fluorescence than that of Tac-G5/2b (Fig. 3*E*). The other two deletion mutants, Tac-G5/2bΔ15 and Tac-G5/2bΔ36, also exhibited robust surface expression (Fig. 3, *B*, *C*, and *E*). Together these results suggest that the ER retention signal(s) is likely embedded in a short sequence, LTCHQRRTQ, in the distal portion of GluR5–2b C terminus.

To determine the precise molecular composition of the ER retention signal, each of the 9 residues (LTCHQRRTQ) (Fig.

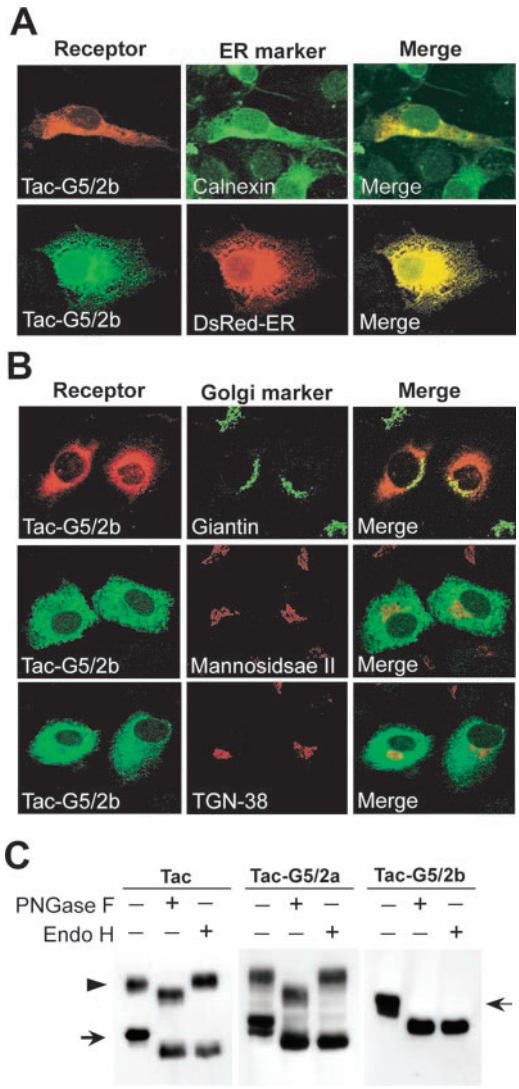

FIG. 2. **Tac-G5/2b receptors are retained in the ER.** *A*, Tac-G5/2b colocalizes with ER markers. In the *top panel*, COS7 cells transfected with Tac-G5/2b were permeabilized and stained with antibodies against Tac (*red*) and the ER marker calnexin (*green*); in the *bottom panel*, COS7 cells were co-transfected with Tac-G5/2b (*green*) and DsRed-ER (*red*). Image overlays show extensive colocalization (*yellow*). *B*, Tac-G5/2b does not localize to Golgi or *trans*-Golgi network compartments. COS7 or NRK cells were transfected with Tac-G5/2b, and co-stained with the Golgi markers, giantin (*green*), mannosidase II (*red*), and TGN-38 (*red*). Image overlays showed no colocalization (*yellow*) in all staining. *C*, ER retention of Tac-G5/2b demonstrated by deglycosylation assays. Tac-G5/2b is sensitive to deglycosylation by endo H, indicating that it is retained in the ER. In contrast, Tac and Tac-G5/2a acquire endo H resistance upon ER exit, although they remain sensitive to PNGase F, which is not compartment-selective. *Arrows* designate immature species, whereas *arrowhead* designates the mature form.

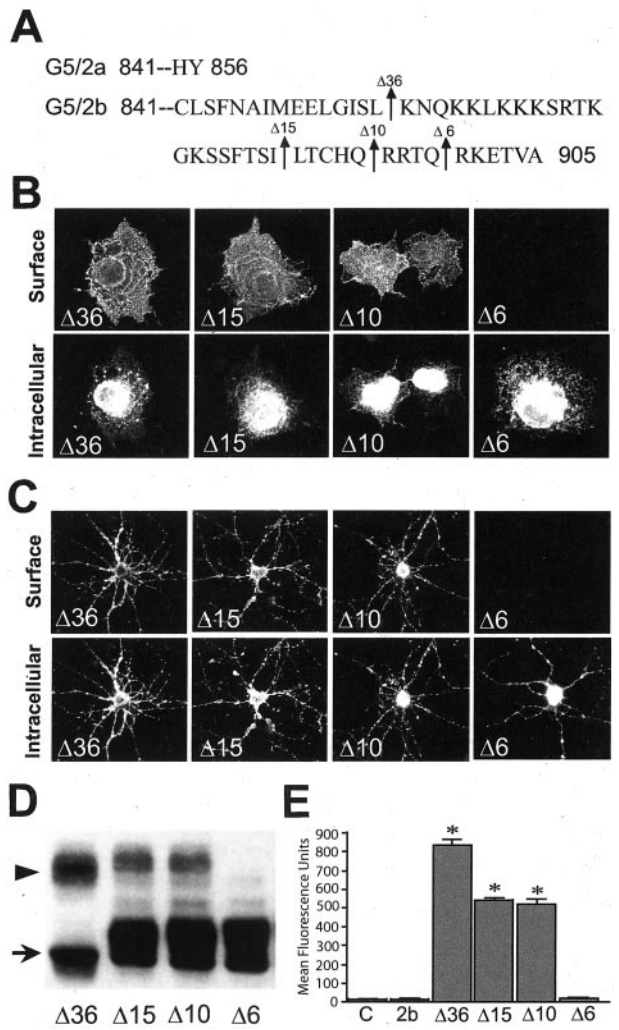

FIG. 3. **Identification of the molecular determinants of Tac-G5/2b ER retention by sequential C-terminal deletions.** *A*, sequence alignment between the C-terminal domains of GluR5–2a and GluR5–2b. The *dashed lines* represent the sequence identical in both; *arrows* indicate the points of truncation used to generate the deletion mutants. *B*, surface and intracellular expression of Tac-G5/2b deletion mutants in COS cells. Deletions of the last 10, 15, or 36 residues, but not the terminal 6 amino acids, induce surface expression of Tac-G5/2b. *C*, the same constructs expressed in hippocampal neurons show identical patterns as in COS cells. *D*, Western blot of Tac-G5/2b deletion mutants. Tac-G5/2bΔ36, Δ15, and Δ10 are present as mature as well as immature species, indicating their egress from ER. The lack of a mature form for Tac-G5/2bΔ6 suggests that it is still ER-retained. *Arrow* designates immature species, whereas *arrowhead* designates the mature form. *E*, flow cytometric quantification for the surface expression of Tac-G5/2b deletion mutants in HEK293 cells. Note that deletion of the last 10 or more residues results in robust surface expression of Tac-G5/2b. Data represent means ± S.E. of fluorescence intensities from 50,000 cells stained for surface expression of Tac-G5/2b and mutants (*, $p < 0.05$ relative to mock-transfected control, by Student's unpaired *t* test).

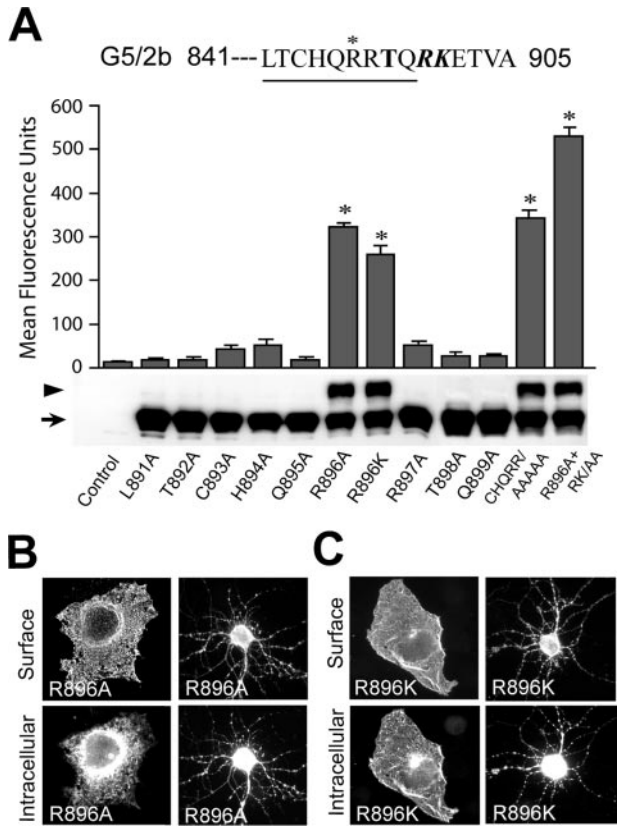

FIG. 4. **Identification of arginine 896 as a critical determinant for ER retention.** *A*, flow cytometric quantification for the surface expression of Tac-G5/2b mutants with alanine (or lysine) substitution. *Top*, the C-terminal sequence subjected to mutational scanning (*underlined*), positions of the critical Arg-896 (*asterisked*), a consensus phosphorylation site (Thr-898, in *bold letters*), and a pair of positively charged residues (in *bold letters* and *italics*). *Middle*, quantification data of receptor surface expression. Note that four mutants, R896A, R896K, CHQRR/AAAAA, and R896A+RK/AA showed robust surface expression, whereas other mutations had no significant effect. Data represent means ± S.E. of fluorescence intensities from 50,000 cells stained for surface expression of the Tac-G5/2b mutants (*, $p < 0.05$ relative to mock-transfected control, by Student's unpaired *t* test). *Bottom*, Western blot of the Tac-G5/2b mutants is shown. All mutants of Arg-896 (R896A, R896K, CHQRR/AAAAA, and R896A+RK/AA) exist as both mature and immature species, indicating their egress from ER. Other mutants remain retained, evident by the lack of a mature form. All wild type and mutant receptors were expressed at comparable levels. *Arrow* designates immature species, whereas *arrowhead* designates the mature form. *B* and *C*, surface and intracellular expression of the R896A (*B*) or R896K mutant (*C*) in COS cells (*left panels*) and hippocampal neurons (*right panels*). Robust surface signals were detected in cell types.

4*A*, *top panel*) was replaced with an alanine. The mutants were then expressed in HEK cells and examined for surface expression using FAC analysis. A robust surface signal was only detected for the R896A mutant (Tac-G5/2b-R896A), whereas other mutations either had no effect (*i.e.* L891A, T892A, Q895A, T898A, and Q899A) or showed an insignificant increase (C893A, H894A, and R897A) (Fig. 4*A*, *middle panel*). Accordingly, no mature form could be detected for any other receptor except the R896A mutant (Fig. 4*A*, *bottom panel*). Furthermore, when expressed in COS cells and hippocampal neurons, Tac-G5/2b-R896A showed strong surface expression (Fig. 4*B*). These data indicate that Arg-896 is essential for the ER retention of the Tac-G5/2b, whereas other residues do not have such a dominant effect. Consistent with this idea, mutating multiple residues surrounding Arg-896 (*i.e.* CHQRR/AAAAA) did not further enhance surface expression. In addition, replacement of Arg-896 with a lysine residue (Tac-G5/2b-R896K) also resulted in robust surface expression, both in heterologous cells (Fig. 4, *A* and *C*) and hippocampal neurons (Fig. 4*C*).

Surface expression of the R896A mutant (Fig. 4*A*), although robust, was significantly lower than that of the deletion mutants Δ10, Δ15, and Δ36 when tested in parallel FAC experiments (data for the deletion mutants not shown in Fig. 4 but equivalent to those in Fig. 3*E*). This is a strong indication that additional trafficking signal(s) may exist in the distal C-terminal region of GluR5–2b. It has been previously reported that positively charged amino acids located 5 or 6 residues from the extreme C terminus can significantly decrease the ER export

rate of transmembrane proteins (17). We therefore examined whether Arg-900 and Lys-901, two residues so positioned in GluR5–2b (Fig. 4*A*, *top panel*), play a role in receptor trafficking. In agreement with our earlier results with the deletion mutant Tac-G5/2bΔ6 (Fig. 3), dual alanine substitution of both Arg-900 and Lys-901 in the Tac-G5/2b construct did not cause ER exit (data not shown). However, surface expression of a Tac-G5/2b(R896A+RK/AA) mutant, which had all three sites substituted (*i.e.* Arg-896, Arg-900, and Lys-901), was significantly higher than that of the R896A single mutant and was comparable with the level shown by Tac-G5/2bΔ10 (Fig. 4*A*, *middle panel*). This is consistent with a scenario that Arg-900 and Lys-901 control the rate at which receptors can exit from the ER, following disruption of the Arg-896-mediated retention. Taken together, these results demonstrate that Arg-896 plays a key role in mediating the ER retention of Tac-G5/2b, whereas Arg-900 and Lys-901 may regulate the kinetics of receptor trafficking.

Arg-896 Is Conserved, but Functionally Disabled in GluR6/7 Subunits—A sequence alignment between the C termini of the GluR5–2b, GluR5–6, and GluR5–7 subunits reveals that Arg-896 is conserved in all three subunits (*i.e.* Arg-899 in GluR6 or Arg-869 in GluR7) (Fig. 5*A*). However, the amino acids surrounding the conserved arginine are identical in GluR6 and GluR7 but share little homology with those in GluR5 (Fig. 5*A*). These differences may impact the function of Arg-896 as an ER retention signal, because GluR6 receptors have been previously shown to express robustly on the cell surface (4).

To test this idea and map other residues important for Arg-896-mediated ER retention, we swapped the residues surrounding the conserved arginine in GluR5–2b and GluR6, and examined their effects on receptor trafficking. When the three amino acids located N-terminal to Arg-899 in Tac-G6 (FND) were replaced with the corresponding residues from Tac-G5/2b (CHQ), the resulting Tac-G6-FND/CHQ became mostly endo H-sensitive (Fig. 5*B*, *bottom panel*) and was barely detectable on the cell surface, as shown by FAC (Fig. 5*B*, *top panel*) and immunostaining (Fig. 5*C*). Consistent with this result, substitution of the CHQ sequence in Tac-G5/2b with FND (Tac-G5-CHQ/FND) conferred onto it the ability to exit from ER (Fig. 5*D*, *lower panel*) and express on the plasma membrane at a comparable level to that of the R896A mutant (Fig. 5*D*, *top panel*, and *E*). In contrast, exchanging residues positioned C-terminal to the conserved arginines (*i.e.* TQR in GluR5 and LPG in GluR6) did not change the expression profile of either receptor (Fig. 5, *B* and *D*). These data clearly indicate that additional residues surrounding Arg-896 are integral elements of a functional motif, and are directly involved in mediating the ER retention of Tac-G5/2b.

Arg-896-mediated ER Retention Is Regulated by a Phosphorylation-mimic Mutation, but Not PDZ Interactions—The C-terminal domain of GluR5–2b contains several consensus sites for serine/threonine protein kinases and was recently shown to be *in vitro* phosphorylated by protein kinase A (PKA) and PKC (12, 18). Because one of the potential sites, Thr-898, is in close proximity to the ER retention motif (Fig. 4*A*, *top panel*), we hypothesized that its phosphorylation might disrupt ER retention and promote surface delivery of the receptor. Indeed, Tac-G5/2b receptors carrying a negative charge mutation to mimic phosphorylation at Thr-898 (Tac-G5/2b-T898E) exhibited significantly increased surface expression in both COS7 cells and hippocampal neurons (Fig. 6*A*). FAC analysis showed that the T898E mutant was expressed at 10-fold higher level on the plasma membrane than Tac-G5/2b (Fig. 6*C*), and the presence of a mature form in Western blots also indicated its egress from the ER. In contrast, a mutation that prevents phosphorylation at the same site (Tac-G5/2b-T898A) showed no effect on surface expression (Figs. 4*A* and 6*B*).

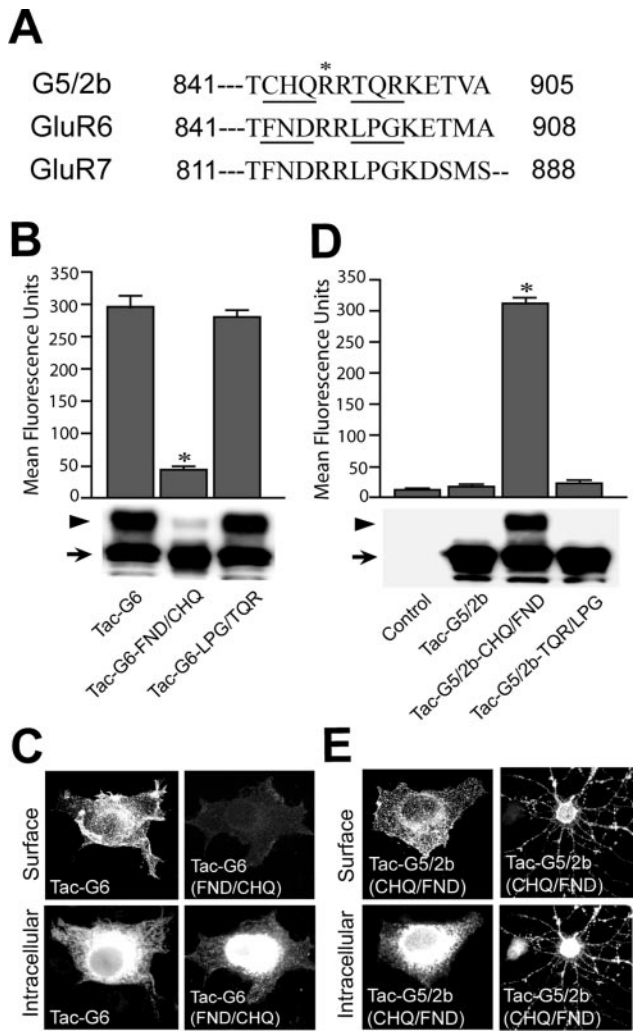

FIG. 5. **Mapping additional sequence determinants for ER retention.** *A*, sequence alignment between C termini of GluR5–2b, GluR6, and GluR7. Note that Arg-896 (*asterisk*) is conserved in all, but the surrounding residues (*underlined*) are distinctly different. *B*, expression profiles of Tac-G6 and mutants. Replacing residues N-terminal to the conserved arginine (FND) with the counterparts from GluR5–2b (CHQ) leads to ER retention of Tac-G6. Conversely, a C-terminal swapping mutant is indistinguishable from the unaltered receptor. *Top*, flow cytometric quantification for the surface expression of Tac-G6 and mutants in HEK293 cells. Data represent means ± S.E. of fluorescence intensities from 50,000 cells stained for surface expression of Tac-G6 and mutants (*, $p < 0.05$ relative to Tac-G6, by Student's unpaired t test). *Bottom*, Western blot of Tac-G6 and mutants. All proteins are expressed equally, but little of the mature form of Tac-G6-FND/CHQ is observed. *Arrow* designates immature species, whereas *arrowhead* designates the mature form. *C*, surface and intracellular expression of Tac-G6 and mutants in COS cells. Tac-G6 (*left*) shows robust surface expression, whereas Tac-G6-FND/CHQ (*right*) has barely detectable surface signal. *D*, expression profiles of Tac-G5/2b and mutants. Replacing residues N-terminal (but not C-terminal) to Arg-896 (*i.e.* CHQ but not TQR) with the counterparts from GluR6 leads to ER exit of Tac-G5/2b. *Top*, flow cytometric quantification for the surface expression of Tac-G5/2b and mutants in HEK293 cells. Tac-G5/2b-CHQ/FND shows robust surface expression similar to that of the R896A mutant. Data represent means ± S.E. of fluorescence intensities from 50,000 cells stained for surface expression of Tac-G5/2b and mutants (*, $p < 0.05$ relative to mock-transfected control, by Student's unpaired t test). *Bottom*, Western blot of Tac-G5/2b and mutants. All proteins are expressed equally, but only the Tac-G5/2b-CHQ/FND acquires the mature form. *Arrow* designates immature species, whereas *arrowhead* designates the mature form. *E*, staining of Tac-G5/2b-CHQ/FND expressed in COS cells (*left*) and hippocampal neurons (*right*). Strong surface expression was detected in both cell types.

To determine whether endogenous protein kinases can phos-

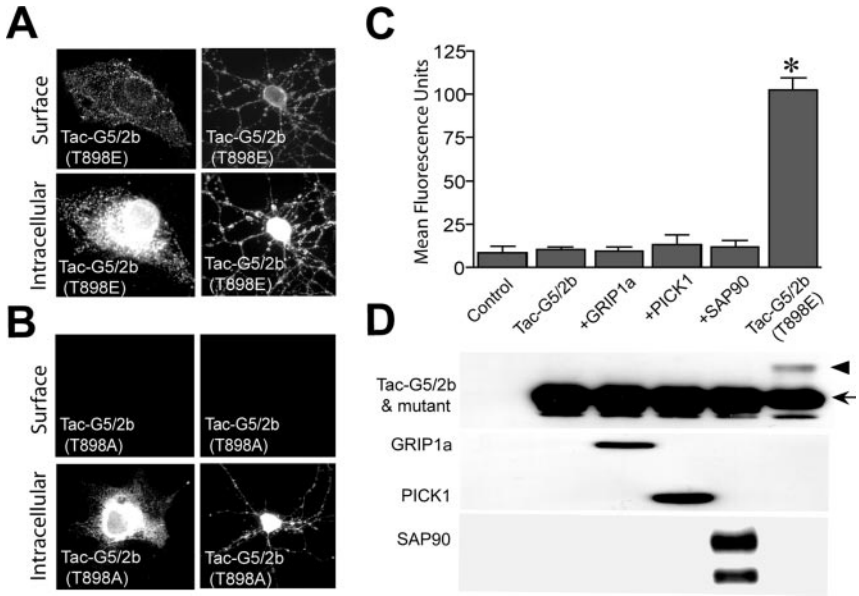

FIG. 6. **A phosphorylation-mimic mutation, but not PDZ interactions, reverses ER retention.** *A*, suppression of Tac-G5/2b ER retention by a phosphorylation-mimic mutation of Thr-898. Surface and intracellular expression of Tac-G5/2b-T898E in COS cells (*left panels*) and hippocampal neurons (*right panels*) is shown; surface signals were readily detectable in both cell types. *B*, conversely, alanine substitution of Thr-898 does not affect ER retention. Surface and intracellular expression of Tac-G5/2b-T898A in COS cells (*left panels*) and hippocampal neurons (*right panels*) is shown. No surface signal was detected. *C*, interactions with PDZ-containing proteins do not relieve ER retention of Tac-G5/2b. Tac-G5/2b-T898E shows surface expression by FAC analyses, but Tac-G5/2b coexpressed with PDZ proteins does not. HEK293 cells were transfected with Tac-G5/2b-T898E alone, or Tac-G5/2b together with PDZ proteins as indicated. Data represent means ± S.E. of fluorescence intensities from 50,000 cells stained for surface expression (*, $p < 0.05$ relative to mock-transfected control, by Student's unpaired t test). *D*, Western blot shows that all proteins express well, but a mature form can only be detected for the Tac-G5/2b-T898E mutant (*top panel*, *sixth lane*). *Arrow* designates immature species, whereas *arrowhead* designates the mature form.

phorylate Tac-G5/2b and promote its release from the ER, transfected COS7 or HEK cells were treated with either the cell-permeable PKC activator phorbol ester (phorbol 12-myristate 13-acetate, 100 nM, 0.5 h) or the PKA activator forskolin (50 μM, 2 h) together with a phosphodiesterase inhibitor isobutylmethylxanthine (10 μM). These treatments have been reported to inhibit RXR-mediated ER retention through PKC- or PKA-dependent receptor phosphorylation (7, 19). However we were unable to observe, by immunostaining and FAC analysis, enhanced surface expression of Tac-G5/2b after either treatment.

The C-terminal domains of GluR5–2b and GluR5–2c, but not GluR5–2a, contain consensus type I PDZ-binding sequences near the ER retention motif, which can interact directly with a number of PDZ-containing proteins (12). Although deletion of the last 6 amino acids in Tac-G5/2b (including the PDZ-binding sequence ETVA) did not affect its ER retention (Fig. 3), PDZ interactions may still be able to play a regulatory role in receptor trafficking as reported for the NMDA receptor subunit NR1 (6, 7). We therefore examined the effect of three different PDZ proteins: PSD-95/SAP90 (postsynaptic density-95/synapse-associated protein 90), PICK (protein interacting with C kinase), and GRIP (glutamate receptor-interacting protein), all of which have been shown previously to interact with the C terminus of GluR5–2b (12). When co-expressed individually with Tac-G5/2b, these proteins had no detectable effect on Tac-G5/2b trafficking, which was still retained intracellularly (Fig. 6, *C* and *D*).

Arg-896-mediated ER Retention Regulates GluR5 Receptor Function—To determine whether this putative ER retention motif can regulate trafficking or function of homomeric GluR5–2b receptors, we compared the surface expression of the wild type receptor with a mutant, GluR5–2b(R896A). When expressed in COS7 cells, GluR5–2b showed weak but detectable surface labeling (Fig. 7, *A* and *B*) in most transfected cells, whereas quantitative Western blotting analyses indicated that its expression level was significantly lower than that of Tac-G5/2b chimera (Fig. 7, *C* and *D*). Therefore, the surface signal of GluR5–2b can not be explained by overexpression; rather, it is more likely that the ER retention signal identified with the Tac-G5/2b reporter exerts a weaker effect on the fully assembled oligomeric receptors. Despite these differences, the full-length R896A mutant did exhibit much greater (~2.5-fold increase) surface expression compared with the wild type receptor (Fig. 7, *A* and *B*), whereas Western blot analyses showed equivalent levels of protein expression (Fig. 7*B*, *bottom panel*). We further examined the effect of residues Arg-900 and Lys-901, which appear to control the ER export rate of Tac-G5/2b (Fig. 4*A*). When both amino acids were replaced with alanines, the resulting GluR5–2b(RK/AA) mutant showed a similar increase in surface labeling (Fig. 7*B*). Finally, the receptor with all three sites mutated, GluR5–2b(R896A+RK/AA) demonstrated the highest level (~4-fold increase) of surface expression (Fig. 7*B*).

Consistent with the biochemical results, increased functional expression of GluR5–2b receptors was observed in patch-clamp recordings from HEK293 cells expressing the mutant receptors (Fig. 8). Glutamate-evoked currents had a mean peak amplitude of 0.67 ± 0.20 nA in cells expressing GluR5–2b ($n = 10$), whereas mean current amplitudes in the cells expressing the trafficking mutants were >4-fold larger (GluR5–2b(896A): 2.76 ± 0.62 nA; GluR5–2b(RK/AA): 2.44 ± 0.39 nA; GluR5–2b(R896A+RK/AA): 3.75 ± 0.70; $n = 11$ for each mutant) (Fig. 8*A*; $p < 0.05$ compared with wild type). In addition to increased amplitudes, the trafficking mutants also had altered rates of desensitization compared with wild type GluR5–2b receptors (Fig. 8*B*). Desensitization in the wild type receptor was highly variable (mean $\tau_{des} = 5.2 \pm 1.0$ ms, $n = 8$), as was seen previously for GluR5–2a receptors expressed in HEK cells (20). In contrast, currents from the mutants were rapidly desensitizing, with the triple mutant GluR5–2b(R896A+RK/AA) having the fastest τ_{des} (2.05 ± 0.26, $n = 11$, $p < 0.05$ compared with

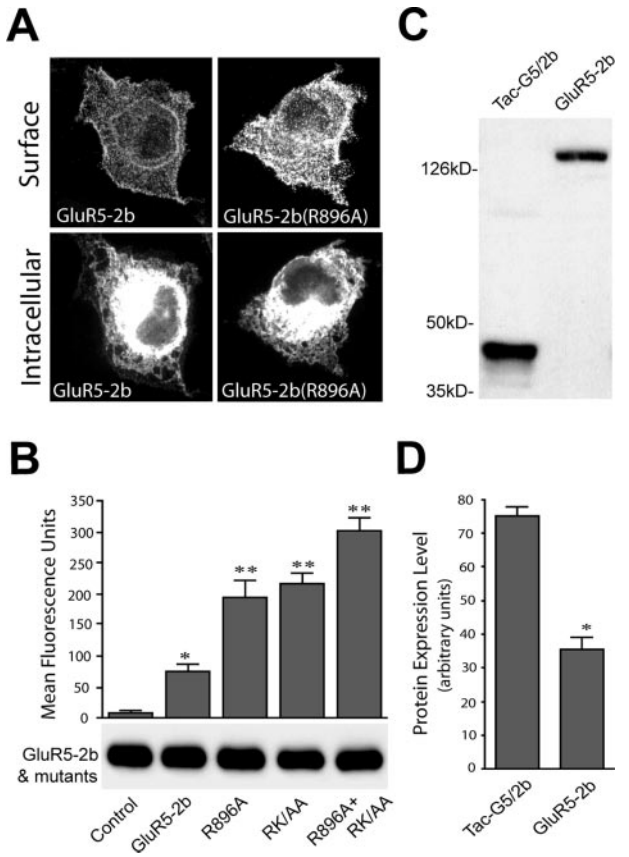

FIG. 7. **ER retention is a rate-limiting factor for the surface expression of homomeric GluR5–2b receptors.** *A*, disruption of the ER retention signal leads to increased surface expression of GluR5–2b. Immunocytochemical analysis of GluR5–2b (*left panels*) and a R896A mutant (*right panels*) expressed in COS cells indicates a much stronger surface signal for the mutant. *B*, flow cytometric quantification for the surface expression of GluR5–2b and mutants in HEK293 cells. *Top*, cells expressing GluR5–2b(R896A) or GluR5–2b(RK/AA) have ~2.5-fold higher surface fluorescence than that of GluR5, whereas GluR5–2b(R896A+RK/AA) shows a 4-fold increase. Data represent means ± S.E. of fluorescence intensities from 50,000 cells stained for surface expression of wild type and mutant GluR5–2b receptors (*, $p < 0.05$ relative to GluR5–2b minus primary antibody control; **, $p < 0.05$ relative to GluR5–2b, by Student's unpaired *t* test). *Bottom*, Western blot shows that all proteins are expressed at comparable levels. *C* and *D*, differential expression of GluR5–2b and Tac-G5/2b in COS cells. A representative Western blot (*C*) and quantitative analyses (*D*) show that GluR5–2b is expressed at a lower level compared with the Tac-G5/2b chimera (*, $p < 0.05$). Note that both the wild type and mutant GluR5 receptors are tagged at the N terminus with GFP.

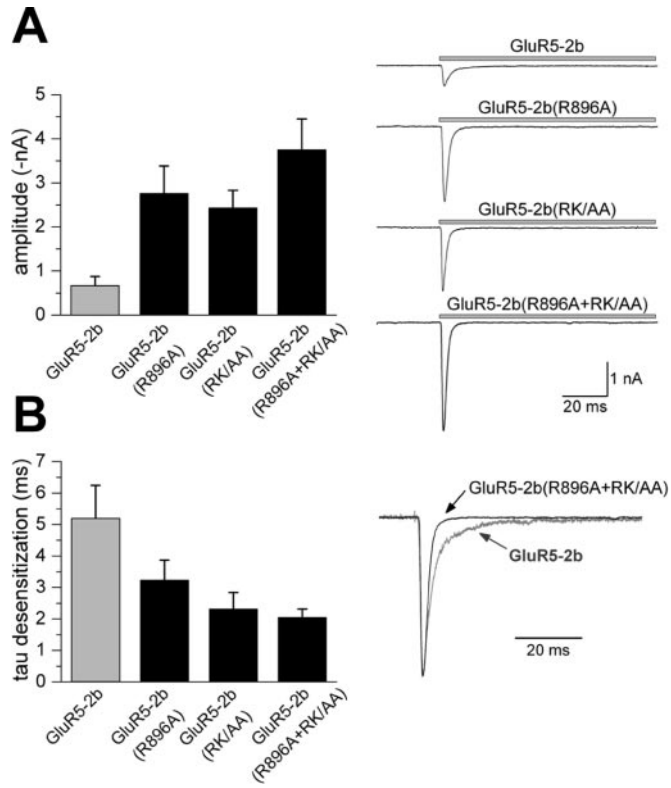

FIG. 8. **Mutation of residues comprising the trafficking motifs increases functional expression and the rate of desensitization of GluR5–2b receptors.** *A*, increased current amplitudes from mutant GluR5–2b receptors. The *graph* shows the mean peak amplitudes from glutamate-evoked currents elicited from HEK293 cells expressing GluR5–2b, GluR5–2b(R896A), GluR5–2b(RK/AA), and GluR5–2b(R896A+RK/AA) receptors. Mean amplitudes from the mutant receptors were significantly larger than that from GluR5–2b receptors ($p < 0.05$, by Student's unpaired *t* test). Representative whole-cell currents are shown on the *right side* of the *panel*. Glutamate (10 mM) was applied for 100 ms (*gray bar*). *B*, rapid desensitization rates of currents from GluR5–2b mutants. The *graph* shows the mean time constant of desensitization for glutamate currents from the wild type and mutant receptors. Current decays in the presence of glutamate were well fit with a single exponential function in most cases. The τ_{des} was significantly faster for the mutant receptors ($p < 0.05$). In the *right panel*, the time courses of current decays are compared. The representative current trace from GluR5–2b receptor was normalized to the peak amplitude of the GluR5–2b(R896A+RK/AA) current trace to facilitate this comparison.

GluR5–2b). These results demonstrate that Arg-896, Arg-900, and Lys-901 confer intracellular retention of the intact GluR5–2b receptors, and that elimination of these sites increases functional expression as well as altering receptor kinetics.

DISCUSSION

The controlled surface expression of ionotropic glutamate receptors plays a key role in regulating neuronal function. In particular, the insertion and removal of receptors provide an important mechanism for modifying the strength of excitatory synapses (21). AMPA receptor subunits employ distinct mechanisms to regulate proximal and distal trafficking processes, involving a variety of kinases and PDZ-containing proteins (8, 22, 23). Other studies demonstrate that multiple trafficking signals also exist to control the surface expression of NMDA receptors (5–7, 24). In the case of kainate receptors, although progress has been made in understanding certain synaptic trafficking events (12, 18), little is known about the mechanisms regulating subunit assembly and maturation through the secretory pathway. We have recently discovered an arginine-rich ER retention signal and a dileucine endocytic motif controlling surface expression of the KA2 subunit (4). Here we report the identification of a novel ER retention signal in the C-terminal domain of the GluR5 splice variant, GluR5–2b. Disruption of this signal, which consists of Arg-896 and surrounding residues, allows ER exit and maturation of a Tac-G5/2b reporter and results in significant increases in the surface expression of homomeric GluR5–2b receptor, indicating that ER retention indeed plays a rate-limiting role in GluR5 receptor trafficking.

A Novel Mechanism Regulating GluR5 Trafficking—ER retention/retrieval may serve as an important checkpoint for the surface delivery of multimeric transmembrane proteins, ensuring that only fully assembled functional complexes are expressed on the plasma membrane (3). The unassembled and/or misfolded subunits are retained in the ER, and may be further targeted for degradation by ubiquitination and cleavage in the proteasomes (25, 26). The ER retention/retrieval process can be initiated through the recognition of discrete retention signals

or protein misfolding. The best characterized ER retention signals are the luminal H/KDEL sequence and cytoplasmic KK*XX* motif (3). Recent studies have revealed additional ER retention signals, including a cytoplasmic R*X*R-type sequence (6, 7, 27, 28) and a number of transmembrane motifs (8, 29).

In this study, we demonstrate that the C-terminal domain of a GluR5 receptor splice variant, GluR5–2b, contains an ER retention signal. Elements of the retention motif were then mapped through mutation analysis of Tac-G5/2b chimeras. This approach has been used extensively for the identification of trafficking signals in the secretory pathway (30–33). In particular, the monomeric nature of the Tac chimera allows the isolation of trafficking signal(s) that otherwise might be masked during oligomeric assembly (3). We identified Arg-896, a residue conserved in most low affinity kainate receptor subunits, as an essential determinant of this ER retention process. Alanine substitution of this residue induced robust surface expression of the chimeric Tac-G5/2b protein.

Interestingly, this conserved arginine does not confer ER retention in a largely homologous Tac-G6 chimera, suggesting that certain neighboring residues are also critical elements of the retention signal. Indeed, replacing residues preceding Arg-896 in Tac-G5/2b with those in GluR6 is also sufficient to disrupt ER retention and allow receptor surface expression. In addition, mutating a pair of positively charged residues, Arg-900 and Lys-901, further enhances surface expression, likely by increasing the ER export rate of the receptors. However, surface expression of all these mutants is still 30–50% lower than that of Tac-G5/2a (which has the shortest C terminus), suggesting the existence of additional regulatory mechanism(s). The multiple lysine clusters present in the C-terminal domain are likely candidates, because it has been shown that ubiquitination of lysine residues regulates the abundance of GLR-1 glutamate receptors at postsynaptic elements in *C. elegans* (34). Although no similar mechanism has been reported for mammalian ionotropic glutamate receptors, ubiquitination has been shown to control the expression of many synaptic proteins (35). Furthermore, ubiquitin-dependent post-Golgi sorting, endocytosis, and protein degradation have been well documented for various ion channels and G-protein-coupled receptors (26, 36–38). Future studies will address the possibility that ubiquitination regulates kainate receptor trafficking and function.

In contrast to its dominance in the monomeric Tac-G5/2b protein, the Arg-896 retention signal does not confer complete ER retention of the full-length GluR5–2b subunits, which can assemble into functional homomultimeric receptors. Nonetheless, this motif still controls GluR5–2b trafficking because mutating Arg-896 significantly increases the surface expression of functional receptors. The loss of dominance may be attributed to the masking of this ER retention signal in the fully assembled mature receptors. Similar mechanisms have been shown for other proteins, specifically, the ER retention signals in IgE and $GABA_B$ receptors are masked, either by steric hindrance (39) or through specific interaction among the C termini of constituent subunits (28). Alternatively, the reduced effect of Arg-896 in full-length GluR5–2b could be explained by the presence of forward trafficking signals, which may reside either in a different GluR5 domain or in other constituents of the receptor assembly. Indeed, an anterograde trafficking determinant has been identified in the C terminus of the GluR6 subunit.[2] Moreover, the N-terminal domain, certain transmembrane segments, and the extracellular loops are critical for the proper assembly and expression of functional AMPA and kainate receptors (40). Significantly, the other GluR5 isoforms with long C-terminal tails (*i.e.* GluR5–1b, GluR5–2b, and GluR5–2c) also contain this ER retention signal and appear to have weak surface expression.[3] Therefore, it is tempting to propose that Arg-896-mediated ER retention may represent a general mechanism regulating the intracellular trafficking and surface expression of long isoform GluR5 receptors.

Regulation of Arg-896-mediated ER Retention by Phosphorylation and PDZ Interaction—Protein phosphorylation and interaction with PDZ proteins have been reported to regulate ionotropic glutamate receptor trafficking (21, 41). The ER retention of NR1 splice variants can be inhibited by PKC phosphorylation and association with a PDZ protein (6, 7). The distinct trafficking profiles displayed by AMPA receptor subunits also largely rely on their differential phosphorylation by various kinases and interaction with PDZ-containing proteins PICK1, GRIP, and SAP97 (13, 42–45). In addition, phosphorylation has been shown to enhance synaptic delivery of GluR5-containing kainate receptors (12). Further highlighting the complexity of trafficking regulation, phosphorylation can also act as a molecular switch to control a receptor's binding preference for particular PDZ proteins (46). In the present study, we explored whether similar mechanisms are utilized to control GluR5–2b kainate receptor trafficking through the early secretory pathway. Although activation of endogenous PKA or PKC did not appear to increase surface expression of Tac-G5/2b, a phosphorylation-mimic mutation (*i.e.* T898E) near the ER retention signal was shown to promote ER egress and surface delivery of the receptor. Thus, although the data are not conclusive, they do suggest that GluR5–2b trafficking may be regulated by direct phosphorylation.

The PDZ proteins, PICK1 and GRIP, have been implicated in the synaptic delivery of kainate receptors, because both can bind to GluR5–2b and regulate kainate receptor-mediated synaptic current (12). In this study, we examined the effects of these PDZ-mediated protein interactions on the ER retention of Tac-G5/2b. Interestingly, neither changed the intracellular distribution of Tac-G5/2b, nor did PSD-95/SAP90, another PDZ protein previously shown to regulate the clustering and desensitization of GluR6-containing receptors (47). These seemingly conflicting observations could be the result of differences in the regulation of proximal and distal trafficking processes. In support of this idea, stargazin protein was recently shown to be essential for the delivery of AMPA receptors to the plasma membrane, whereas PSD-95/SAP90 is critically involved in their synaptic incorporation (48). It is conceivable that kainate receptors may also employ different regulatory mechanisms in various trafficking steps through the secretory pathway.

Physiological Implications of the ER Retention Signal in Kainate Receptor Function—Although GluR5 transcripts are known to be developmentally regulated (49) and present in a number of neuronal populations (50, 51), the relative abundance of GluR5 isoforms in various brain regions remains undefined. Nonetheless, the existence of an ER retention signal specific to a subset of GluR5 splice variants would have profound implications for kainate receptor assembly and function, by controlling the supply of GluR5-containing kainate receptors to the plasma membrane. Indeed, we find that disruption of the ER retention by mutating Arg-896 can significantly increase (~2.5-fold) the surface expression of GluR5–2b receptors, as well as altering their desensitization properties. In addition, the ER retention signal might also play a role in determining the availability of different GluR5 splice variants for functional assembly. Preferential ER retention of the long

[2] Yan, S., Sanders, J. M., Xu, J., Zhu, Y., Contractor, A., and Swanson, G. T. (2003) *Journal of Neuroscience*, in press.

[3] Z. Ren and J. Marshall, unpublished data.

isoform GluR5 subunits (*i.e.* GluR5–1, GluR5–2b, and GluR5–2c) could create an intracellular reserve pool that ensures their availability for incorporation into functional channels before exiting the ER. Furthermore, these events may directly impact the composition of synaptic kainate receptors, because there is growing evidence supporting local protein synthesis and maturation in the dendrites (52–55).

GluR5 is known, at least in heterologous cells, to assemble into mature heteromeric receptors with other low affinity (GluR6/7) or high affinity (KA1 and KA2) subunits (56, 57). In neurons, the scenario is likely to be far more complex, with multiple subunits and splice variants often coexpressed in the same neuron but forming a broad range of receptors with different subunit compositions (58–61). ER retention and endocytic signals have been recently documented for KA2 (4), whereas an anterograde trafficking determinant was identified in the GluR6 subunit.[2] It will be important for future studies to determine how the ER retention signal in GluR5 may interact with other subunits, as well as to elucidate the relationship between this retention signal and other trafficking motifs within mature kainate receptor complexes.

Acknowledgments—We thank Drs. Peter Seeburg and Steve Heinemann for providing the GluR5 and GluR6 cDNAs, Dr. Richard Huganir for the PICK1 and GRIP1a vectors, and Dr. Morgan Sheng for the PSD-95 construct. We are very grateful to Dr. Leslie Blair for critical reading of the manuscript.

REFERENCES

1. Seeburg, P. H. (1993) *Trends Neurosci.* **16,** 359–365
2. Hollmann, M., and Heinemann, S. (1994) *Annu. Rev. Neurosci.* **17,** 31–108
3. Teasdale, R. D., and Jackson, M. R. (1996) *Annu. Rev. Cell Dev. Biol.* **12,** 27–54
4. Ren, Z., Riley, N. J., Garcia, E. P., Sanders, J. M., Swanson, G. T., and Marshall, J. (2003) *J. Neurosci.* **23,** 6608–6616
5. Okabe, S., Miwa, A., and Okado, H. (1999) *J. Neurosci.* **19,** 7781–7792
6. Standley, S., Roche, K. W., McCallum, J., Sans, N., and Wenthold, R. J. (2000) *Neuron* **28,** 887–898
7. Scott, D. B., Blanpied, T. A., Swanson, G. T., Zhang, C., and Ehlers, M. D. (2001) *J. Neurosci.* **21,** 3063–3072
8. Greger, I. H., Khatri, L., and Ziff, E. B. (2002) *Neuron* **34,** 759–772
9. Bettler, B., Boulter, J., Hermans-Borgmeyer, I., O'Shea-Greenfield, A., Deneris, E. S., Moll, C., Borgmeyer, U., Hollmann, M., and Heinemann, S. (1990) *Neuron* **5,** 583–595
10. Sommer, B., Burnashev, N., Verdoorn, T. A., Keinanen, K., Sakmann, B., and Seeburg, P. H. (1992) *EMBO J.* **11,** 1651–1656
11. Swanson, G. T., Feldmeyer, D., Kaneda, M., and Cull-Candy, S. G. (1996) *J. Physiol.* (*Lond.*) **492,** 129–142
12. Hirbec, H., Francis, J. C., Lauri, S. E., Braithwaite, S. P., Coussen, F., Mulle, C., Dev, K. K., Coutinho, V., Meyer, G., Isaac, J. T., Collingridge, G. L., and Henley, J. M. (2003) *Neuron* **37,** 625–638
13. Leonard, W. J., Depper, J. M., Robb, R. J., Waldmann, T. A., and Greene, W. C. (1983) *Proc. Natl. Acad. Sci. U. S. A.* **80,** 6957–6961
14. Bonifacino, J. S., Suzuki, C. K., and Klausner, R. D. (1990) *Science* **247,** 79–82
15. Trimble, R. B., and Maley, F. (1984) *Anal. Biochem.* **141,** 515–522
16. Tarentino, A. L., Gomez, C. M., and Plummer, T. H., Jr. (1985) *Biochemistry* **24,** 4665–4671
17. Jackson, M. R., Nilsson, T., and Peterson, P. A. (1990) *EMBO J.* **9,** 3153–3162
18. Cho, K., Francis, J. C., Hirbec, H., Dev, K., Brown, M. W., Henley, J. M., and Bashir, Z. I. (2003) *J. Physiol.* (*Lond.*) **548,** 723–730
19. Zhou, J., Shin, H. G., Yi, J., Shen, W., Williams, C. P., and Murray, K. T. (2002) *Circ. Res.* **91,** 540–546
20. Swanson, G. T., and Heinemann, S. F. (1998) *J. Physiol.* (*Lond.*) **513,** 639–646
21. Malinow, R., and Malenka, R. C. (2002) *Annu. Rev. Neurosci.* **25,** 103–126
22. Shi, S., Hayashi, Y., Esteban, J. A., and Malinow, R. (2001) *Cell* **105,** 331–343
23. Zhu, J. J., Qin, Y., Zhao, M., Van Aelst, L., and Malinow, R. (2002) *Cell* **110,** 443–455
24. Roche, K. W., Standley, S., McCallum, J., Dune Ly, C., Ehlers, M. D., and Wenthold, R. J. (2001) *Nat. Neurosci.* **4,** 794–802
25. Keller, S. H., Lindstrom, J., and Taylor, P. (1998) *J. Biol. Chem.* **273,** 17064–17072
26. Keller, S. H., Lindstrom, J., Ellisman, M., and Taylor, P. (2001) *J. Biol. Chem.* **276,** 18384–18391
27. Zerangue, N., Schwappach, B., Jan, Y. N., and Jan, L. Y. (1999) *Neuron* **22,** 537–548
28. Margeta-Mitrovic, M., Jan, Y. N., and Jan, L. Y. (2000) *Neuron* **27,** 97–106
29. Wang, J. M., Zhang, L., Yao, Y., Viroonchatapan, N., Rothe, E., and Wang, Z. Z. (2002) *Nat. Neurosci.* **5,** 963–970
30. Dittrich, E., Haft, C. R., Muys, L., Heinrich, P. C., and Graeve, L. (1996) *J. Biol. Chem.* **271,** 5487–5494
31. Tan, P. K., Waites, C., Liu, Y., Krantz, D. E., and Edwards, R. H. (1998) *J. Biol. Chem.* **273,** 17351–17360
32. Fu, J., and Kreibich, G. (2000) *J. Biol. Chem.* **275,** 3984–3990
33. Aguilar, R. C., Boehm, M., Gorshkova, I., Crouch, R. J., Tomita, K., Saito, T., Ohno, H., and Bonifacino, J. S. (2001) *J. Biol. Chem.* **276,** 13145–13152
34. Burbea, M., Dreier, L., Dittman, J. S., Grunwald, M. E., and Kaplan, J. M. (2002) *Neuron* **35,** 107–120
35. Ehlers, M. D. (2003) *Nat. Neurosci.* **6,** 231–242
36. Cenciarelli, C., Hou, D., Hsu, K. C., Rellahan, B. L., Wiest, D. L., Smith, H. T., Fried, V. A., and Weissman, A. M. (1992) *Science* **257,** 795–797
37. Strous, G. J., van Kerkhof, P., Govers, R., Ciechanover, A., and Schwartz, A. L. (1996) *EMBO J.* **15,** 3806–3812
38. Staub, O., Gautschi, I., Ishikawa, T., Breitschopf, K., Ciechanover, A., Schild, L., and Rotin, D. (1997) *EMBO J.* **16,** 6325–6336
39. Letourneur, F., Hennecke, S., Demolliere, C., and Cosson, P. (1995) *J. Cell Biol.* **129,** 971–978
40. Ayalon, G., and Stern-Bach, Y. (2001) *Neuron* **31,** 103–113
41. Wenthold, R. J., Prybylowski, K., Standley, S., Sans, N., and Petralia, R. S. (2003) *Annu. Rev. Pharmacol. Toxicol.* **43,** 335–358
42. Dong, H., O'Brien, R. J., Fung, E. T., Lanahan, A. A., Worley, P. F., and Huganir, R. L. (1997) *Nature* **386,** 279–284
43. Wyszynski, M., Valtschanoff, J. G., Naisbitt, S., Dunah, A. W., Kim, E., Standaert, D. G., Weinberg, R., and Sheng, M. (1999) *J. Neurosci.* **19,** 6528–6537
44. Osten, P., Khatri, L., Perez, J. L., Kohr, G., Giese, G., Daly, C., Schulz, T. W., Wensky, A., Lee, L. M., and Ziff, E. B. (2000) *Neuron* **27,** 313–325
45. Cai, C., Coleman, S. K., Niemi, K., and Keinanen, K. (2002) *J. Biol. Chem.* **277,** 31484–31490
46. Chung, H. J., Xia, J., Scannevin, R. H., Zhang, X., and Huganir, R. L. (2000) *J. Neurosci.* **20,** 7258–7267
47. Garcia, E. P., Mehta, S., Blair, L. A., Wells, D. G., Shang, J., Fukushima, T., Fallon, J. R., Garner, C. C., and Marshall, J. (1998) *Neuron* **21,** 727–739
48. Chen, L., Chetkovich, D. M., Petralia, R. S., Sweeney, N. T., Kawasaki, Y., Wenthold, R. J., Bredt, D. S., and Nicoll, R. A. (2000) *Nature* **408,** 936–943
49. Bahn, S., Volk, B., and Wisden, W. (1994) *J. Neurosci.* **14,** 5525–5547
50. Wisden, W., and Seeburg, P. H. (1993) *J. Neurosci.* **13,** 3582–3598
51. Good, P. F., Huntley, G. W., Rogers, S. W., Heinemann, S. F., and Morrison, J. H. (1993) *Brain Res.* **624,** 347–353
52. Torre, E. R., and Steward, O. (1996) *J. Neurosci.* **16,** 5967–5978
53. Kacharmina, J. E., Job, C., Crino, P., and Eberwine, J. (2000) *Proc. Natl. Acad. Sci. U. S. A.* **97,** 11545–11550
54. Aakalu, G., Smith, W. B., Nguyen, N., Jiang, C., and Schuman, E. M. (2001) *Neuron* **30,** 489–502
55. Horton, A. C., and Ehlers, M. D. (2003) *J. Neurosci.* **23,** 6188–6199
56. Herb, A., Burnashev, N., Werner, P., Sakmann, B., Wisden, W., and Seeburg, P. H. (1992) *Neuron* **8,** 775–785
57. Cui, C., and Mayer, M. L. (1999) *J. Neurosci.* **19,** 8281–8291
58. Tolle, T. R., Berthele, A., Zieglgansberger, W., Seeburg, P. H., and Wisden, W. (1993) *J. Neurosci.* **13,** 5009–5028
59. Temkin, R., Lowe, D., Jensen, P., Hatt, H., and Smith, D. O. (1997) *Brain Res. Mol. Brain Res.* **52,** 38–45
60. Pemberton, K. E., Belcher, S. M., Ripellino, J. A., and Howe, J. R. (1998) *J. Physiol.* (*Lond.*) **510,** 401–420
61. Paternain, A. V., Herrera, M. T., Nieto, M. A., and Lerma, J. (2000) *J. Neurosci.* **20,** 196–205

Membrane Transport, Structure, Function, and Biogenesis:

Cell Surface Expression of GluR5 Kainate Receptors Is Regulated by an Endoplasmic Reticulum Retention Signal

Zhao Ren, Nathan J. Riley, Leigh A. Needleman, James M. Sanders, Geoffrey T. Swanson and John Marshall

J. Biol. Chem. 2003, 278:52700-52709.
doi: 10.1074/jbc.M309585200 originally published online October 3, 2003